Titan's diverse landscapes as evidenced by Cassini RADAR's third and fourth looks at Titan

J.I. Lunine, C. Elachi, S. D. Wall, M. D. Allison, Y. Anderson, R. Boehmer,
P. Callahan, P. Encrenaz, E. Flamini, G. Franceschetti, et al.

HAL Id: hal-00319753
https://hal.science/hal-00319753

CASSINI RADAR'S THIRD AND FOURTH LOOKS AT TITAN

J.I. Lunine,[1,2,3] C. Elachi[3, 19], S. D. Wall[3], M. D. Allison[4],Y. Anderson[3], R. Boehmer[3], P. Callahan[3], P. Encrenaz[5], E. Flamini[7], G. Franceschetti[7], Y. Gim[3], G. Hamilton[3], S. Hensley[3], M. A. Janssen[3], W. T. K. Johnson[3], K. Kelleher[3], R. L. Kirk[8], R. M. Lopes[3], R. Lorenz[2, 20], D. O. Muhleman[9], R. Orosei[15], S. J. Ostro[3], F. Paganelli[3], Paillou, P.[16], G. Picardi[10], F. Posa[11], J. Radebaugh[2], L. E. Roth[3], R. Seu[10], S. Shaffer[3], L. A. Soderblom[8], B. Stiles[3], E.R. Stofan[12], S. Vetrella[6], R. West[3], C. A. Wood[13], L. Wye[14], H. Zebker[14], G. Alberti[17] E. Karkoschka[2] B. Rizk[2], E. McFarlane[2], C. See[2], and B. Kazeminejad[18].

[1] INAF-IFSI, 00133, Rome, Italy, [2]Lunar and Planetary Laboratory, University of Arizona, Tucson, AZ 85721, U.S.A., [3] Jet Propulsion Laboratory, California Institute of Technology, Pasadena, CA 91109. U.S.A., [4] Goddard Institute for Space Studies, National Aeronautics and Space Administration New York, NY 10025, U.S.A., [5]Observatoire de Paris, 92195 Meudon, France, [6]Agenzia Spaziale Italiana, 00131 Rome, Italy,[7]Facoltá di Ingegneria, 80125 Naples, Italy, [8] U. S. Geological Survey, Flagstaff, AZ 86001, U.S.A, [9] Division of Geological and Planetary Sciences, California Institute of Technology, Pasadena, CA 91125, U.S.A.,[10] Universitá La Sapienza, 00184 Rome, Italy,[11] INFM and Dip. Interateneo di Fisica, Politecnico di Bari, 70126 Bari, Italy, [12] Proxemy Research, Rectortown,VA 20140, U.S.A., [13] Planetary Science Institute, Tucson, AZ 85719, U.S.A., [14] Stanford University, Stanford, CA 94305, USA,[15]CNR-IASF, 00133, Rome, Italy, [16]Observatoire Aquitain des Sciences de l'Univers, UMR 5804, 2, rue de l'Observatoire, BP 89, 33270, Floirac, France. [17]CO.RI.S.T.A., via J.F. Kennedy 5, 80125 Naples, Italy, [18]European Space Technology Center, ESA, Noordwijk, The Netherlands,, [19]now at Space Department, Johns Hopkins University Applied Physics Lab, 11100 Johns Hopkins Road, Laurel, MD 20723, USA. [20]RADAR Team Leader.

Address correspondence to

Jonathan I. Lunine
Lunar and Planetary Lab/U. Arizona
1629 E University Blvd.
Tucson AZ 85721 USA

520 621 2789
520 626 8250 (fax)

Running title:

Cassini radar on Titan

Abstract

Cassini's third and fourth radar flybys, T7 and T8, traversed diverse terrains in the high southern and equatorial latitudes, respectively. The T7 synthetic aperture radar (SAR) swath is somewhat more straightforward to understand in terms of a progressive poleward descent from a high, dissected, and partly hilly terrain down to a low flat plain with embayments and deposits suggestive of the past or even current presence of hydrocarbon liquids. The T8 swath is dominated by dunes of what are likely organic solids, but also contain somewhat enigmatic, probably tectonic, features that may be partly buried or degraded by erosion or relaxation in a thin crust. The dark areas in T7 show no dune morphology, unlike the dark areas in T8, but are composed of a similar material as suggested by a relationship between radar dark/radiometrically warm like that seen in the dunes. The Huygens landing site lies on the edge of the T8 swath; correlation of the radar and Huygens DISR images indicates that to the north of the landing site sit two large longitudinal dunes. Indeed, had the Huygens probe trajectory been just 10 kilometers north of where it actually was, images of large sand dunes would have been returned in place of the fluvially-dissected terrain actually seen—illustrating the strong diversity of Titan's landscapes.

I. Introduction

The Cassini Titan RADAR Mapper is a K_u-band (13.78 GHz frequency; 2.17 cm wavelength) linearly polarized RADAR instrument capable of operating in synthetic aperture (SAR), scatterometer, altimeter and radiometer modes. Here we report on data acquired during two recent passes, referred to as T7 and T8, on September 7 and October 28 (Universal time dates), 2005, respectively. In contrast with the previous Ta and T3 opportunities, these were southern hemisphere passes, and in particular, T7 imaged areas at high southern latitude (Fig. 1 and Table 1). T7 comprises an area less than a third that of T8 (0.6% versus 2% of Titan's surface) in part because a problem external to the radar interrupted onboard recording of the T7 data after the midpoint of the pass.

In this paper we compare the two radar passes, which are strikingly different in terms of terrains and radiometric properties, extend the maps of radar units developed from Ta and T3 in another paper (Stofan *et al.* 2006), and infer the nature of processes that formed various features. While the most striking and recognizable structures in Ta and T3 are, respectively, a volcanic edifice (Lopes *et al.* 2006) and two impact craters, the dominant recognizable features in T7 and T8 are, respectively, channels and dunes.

As in the first two passes, there are large areas of enigmatic and ambiguous terrains in both T7 and T8. By combining results from radiometry and synthetic aperture imaging (SAR), it is possible to compare the dark dune terrain and the smooth, apparently dune-free dark area at the end of T7 in terms of material properties (Paganelli *et al.* 2006). The two passes, paired by proximity of their flyby dates, could not be more different from each other; they reinforce the impression from earlier flybys that Titan's surface is worked by a range of geologic processes, not dominated by one in particular, and in this respect is much like Earth.

In this paper, we consider first the morphologies seen in the SAR imagery from T7 and T8, in section 2 drawing a general picture of the nature of each region and in section 3 considering in more detail various processes evident in the T7 and T8 SAR imagery. In section 4 we review the evidence from radiometric data that the T7 dark plain is similar to the dune fields seen in T3 and T8, and use this along with the radar properties units identified in Stofan *et al.* (2006) to delve deeper into the nature of the T7 dark area in particular. In section 5 we discuss how DISR data and radar data were overlaid to identify the Huygens landing site in T8 SAR imagery. Section 6 provides a comprehensive interpretation of the processes shaping the T7 and T8 swaths, and closes with questions raised by the two passes that will need to be addressed by future data sets.

2. Description of T7 and T8 terrains

The two swaths are displayed as a set of jpeg quadrangles in Figs. 2 (T7) and 3 (T8). The full swaths are, at the time this paper goes to press, released in various formats on the Planetary Data System home page.

2.1 T7

The swath begins in the mid-southern latitudes and proceeds in a south- to southeasterly- direction for some 1970 km. Illumination of the swath is from the top of the strip downward, that is, roughly toward the southwest. The image resolution begins at about 740 meters, improving to 300 meters in azimuth and 450 m in range at the poleward end of the strip near closest approach. The asymmetric nature of the resolution, in contrast to other passes, is an artifact of the loss of the second half of the radar pass. The strip width is 304 km at the equatorward end, and 113 km at its narrowest point.

An area of moderate radar reflectivity characterizes the equatorward edge of the strip and presents a mottled appearance with faint circular features that seem more characteristic of T8 than of the rest of T7. This terrain quickly gives way to a complex of topographically elevated features distinguished by the obvious illumination and shadowing associated with the radar beam (Fig. 2a). These "hills" are arranged in a roughly semicircular fashion around an area of roughly two or three thousand square kilometers. The lack of closure of the hills to the north, the presence of a similarly incomplete but much smaller (roughly 8 km diameter) oval toward the middle, and the lack of distinct topographic features in the darker material enclosed by the semi-circle, suggests that the hills are the remnant of a more extensive structure that has been partially buried and/or eroded. The debris responsible could have been eroded off the hills by rainfall, as is seen at the Huygens landing site in DISR images (Tomasko *et al.* 2005), or deposited as sedimenting aerosols. The fact that the radar-dark material is not very radar-dark compared with that seen in parts of other swaths (Elachi et al., 2005) hints that the overall terrain may be fairly rough, consistent with but not requiring an erosional interpretation (for example, unconsolidated aerosols directly deposited from the atmosphere might be radar bright as well).

Proceeding poleward, past a break in the radar strip on the edge of which may be another (but more poorly defined) circular set of hills, the landscape becomes dissected by a set of channels running roughly poleward from 45°S. The radar return is brighter where the channels fan out more extensively, suggesting deposition of debris (Fig. 2b). The brighter debris fields seem to be truncated by some process—perhaps a change in topographic gradient—that is not evident in the images, so that the terrain becomes radar-dark (and hence possibly smoother) again. Beyond the dark region, however, more channels appear. In some cases channels can be traced for hundreds of kilometers through the transition from darker-to-brighter-to-darker terrain, but there are few of these features, and their courses seem independent of the fan-shaped channel systems (Fig. 2c).

At about 55°S more numerous channels are located in an irregularly shaped bright area of roughly 40,000 square kilometers with no apparent topographic control, against which the channels become dark and appear to broaden out (Fig. 2d). Dark patches, each about 10 km in linear extent and separated by smaller, very bright spots, exist along the western margin of the bright area; the contrast between the dark patches and the bright

spots is the largest in T7 and among the largest in any of the four passes to date. The bright spots have the appearance of being topography illuminated by the beam, but if these are hills they are not organized in any obvious fashion.

The bright area ends southward of 60° S latitude in a terrain with a faint east-west trending texture, the latter continuing poleward about 40 km into a dramatic landscape of semicircular, scalloped terrain that truncates in embayments of a much darker, very subtly modulated terrain (Fig. 2e). This dark area is the highest resolution part of the radar swath, yet no well-defined features can be seen beyond a subtle, patchy variation in brightness. The brighter highlights in the scalloped terrain appear to be hills of relatively low relief that outline the topographic impediments to the embayed material. It is possible that the scalloped terrain extends further equatorward than is apparent in the images, because it has been partially buried by the material in Fig. 2e with the east-west trending texture.

The overall impression generated by the T7 data is that of a landscape that is descending in elevation toward the pole, dissected by rain- or spring-fed fluvial channels, and ending in a now- or recently-wet high-latitude basin bordered by scalloped and embayed terrain. Basic physical conditions in Titan's atmosphere, the meteorological conditions at the Huygens landing site (Niemann *et al.* 2005), and the appearance of the channels themselves as being cut by low viscosity fluids argue for liquid methane, or secondarily liquid ethane, as the working erosive fluid in the channels and –if wet—the dark, nearly featureless terrain closest to the pole.

2.2 T8

This swath spans over three times the surface area covered by T7, and presents a very different set of geologic features. The swath begins just south of the equator and progresses east some 5,000 km. Illumination of the swath is from the top of the strip downward, that is, toward the south, with an incidence angle of the radar beam varying between 18° and 20° near the center of the pass. The image resolution is about 1km at each end of the strip, improving in the center to 300 meters in azimuth and 450 m in range. The swath width is 450 km at the usable edges, narrowing down to 180 km near the center.

The western edge of the swath consists of a poorly defined set of bright and dark patches, within which radar-dark, longitudinal dunes (Lorenz *et al*. 2006) become increasingly apparent toward the east. The contrast between brighter and darker patches increases as well, although it is not clear whether this is an effect of the decreasing distance of the radar from Titan or a real surface contrast; a few very dark, short channels seem to cut across some of the brighter terrain (Fig. 3a). About 1400 km east of the start of the swath, an extensive area of dark, regular dunes appear (Fig. 3b). These dominate the landscape, parting and rejoining around isolated bright obstructions in the field for some 1700 kilometers until they are interrupted by two obstructions each about 100 km in extent (Fig. 3c). To the east of these lies perhaps the most enigmatic area in the two SAR strips. A series of roughly east-west trending hills, whose topographic amplitude from radarclinometry is a few hundred meters, (Radebaugh *et al.* 2006), are interspersed with a variety of vaguely circular features and dark, dune-filled basins (Fig. 3d). East of this

terrain are a few faint fractures or fluvial channels (Fig. 3e), beyond which more extensive dune fields resume again near the northeastern end of the pass.

The overall impression of the T8 region is that of a much less coherent set of morphological signatures than in T7, although this could be an artifact of the much greater areal extent of T8 compared to T7. It is clear that, in the equatorial 2% of Titan covered by T8, fields of longitudinal dunes dominate (Lorenz *et al.* 2006). But what is unclear is the geological origin of the crustal structures that are partly buried by the dunes. The circular features east of the main dune field have a variety of morphologies, some seemingly associated with the hilly topography, others not. Some appear to be partly buried. The largest, which is well to the east of the ridges, possessing a diameter of roughly 60 km, is not much smaller than the impact crater Sinlap (Elachi *et al.* 2006), and yet exhibits none of the crisp topography and contrast that the latter possesses. Specific morphological differences between these circular features and previously identified impact craters include lack of a well-defined rim or surrounding ejecta blanket.

The end of the T8 radar swath includes the Huygens landing site. Colocation of the Huygens DISR and radar data provided a definitive set of coordinates for the site of minus10.4^{o}N, 192.4^{o}W. The collocation process depended on the existence of a set of well-defined dunes in the radar strip also seen in DISR imager; see section 5.

3. Processes seen in the T7 and T8 data sets

In this section we consider a variety of processes previously identified in radar passes (Elachi *et al.* 2005, 2006), VIMS data (Sotin *et al.* 2006), and Huygens DISR imagery (Tomasko *et al.* 2005). In some cases, identification of features with a particular process is provisional or ambiguous, and may remain so until higher resolution data become available from future missions.

3.1 Fluvial Features

Prior to the Huygens probe descent, the Cassini RADAR detected potential fluvial features on the October 2004 TA encounter at around 50°N. This first SAR image of Titan's surface showed some narrow, radar-bright, sinuous features a few tens of km long and less than 1km wide which were interpreted as possible canyons (Elachi *et al.* 2005), in two cases joining with bright triangles that may be alluvial fans. Such an interpretation appears consistent with the striking observation by the Huygens probe (at about 10°S) of rounded cobbles at an apparently alluvial landing site (Tomasko *et al.* 2005) and of fluvial networks with channels some tens of meters across and around 10 km long.   In both the above sets of features, the orientations appeared to be controlled by local hillside slopes.

Rather larger fluvial networks (one sparse and dendritic with channels a few kilometers across, and another denser, braided network) up to 200km long were observed on T3 (Elachi *et al.* 2006) at latitudes of about 20°N. Both networks, on either side of the Menrva impact structure, appear to flow in a northeasterly direction, away from the broad, bright region Xanadu, hinting at a possible regional slope. All of these channels

appear shallow in the images, like desert washes or wadis, lacking any apparent topographic expression (although the radar's limited spatial resolution could admit possible incision depths of a few tens of meters).

In sharp contrast, in T7 are observed a number of rather deeply incised channels. One region, around 40^oS is characterized by a dense network of channels, while further south, one or two channels make their way southeastwards towards the 'shoreline'. Radarclinometry suggests the channels in T7 may be up to 100 m deep with fairly consistent widths; that is, they do not seem to be the large-scale end of a cascade of channel sizes that extend to below the radar resolution of roughly ½ km.

It is noteworthy that the orientation of the channels is consistent with that of T3, in the sense of being toward the east and the pole, and therefore away from Xanadu, consistent with that feature being an elevated region. If so, channels radiating in other directions away from Xanadu may be found in future observations.

In a couple of locations, the channels are rather straight, in one case appearing to form a boundary between a generally radar-brighter substrate to the west and a slightly darker region to the east. Such a straight edge suggests some sort of structural control on the channel.

Dendritic features of another character, broad and radar-dark, were seen further south (poleward) in T7. Lacking topographic expression, one cannot tell if they are channels – they may even be slightly built-up or leveed flows. The radar-dark but speckled appearance suggests they are smooth. Therefore it is tempting to speculate that these are distributary channels that have deposited material that was chiseled out of the channels closer to the equator. The fine-grained materials created in this process may also be a source of the 'sand' forming the dunes and cat scratches.

The T8 swath, between about 5 and 12^oS, presents an altogether different picture, with essentially no fluvial features at all. A couple of short, narrow, potential channels are suggested, but these are unremarkable in orientation or association with other features. The segment of the T8 swath covering the Huygens landing site is of relatively poor resolution (~1km) and the channels observed by Huygens could not be detected.

The fluvial features observed to date and their meteorological context are discussed in more detail elsewhere (Lorenz *et al.* 2006), though it is worth mentioning that the most prominent fluvial features are found at midlatitudes, where the global circulation model (GCM) of Rannou *et al.* (2006) suggests massive (terrestrial day-long, covering 5% of Titan's disk) methane storms during summer.

3.2 Lacustrine features

A number of generally crescent-shaped, 20km dark spots were observed on Ta, together with an irregular archipelago of dark patches nicknamed 'Sissi the Halloween Cat' in Elachi et al. (2005). Lorenz *et al.* (2005) considered the possibility that these features might be lakes given their morphology and radar reflectivity. However, such an interpretation is not unique – patches of solid but smooth material could produce the same appearance.

T7 brought the highest-latitude SAR coverage to date. At high southern latitudes, the character of the surface changes profoundly from a somewhat bright region dissected by the various channels described above to a nearly uniformly dark region. The boundary between them appears scalloped and cuspate, like that of some estuarine shorelines on

Earth. Unfortunately, the premature truncation of the T7 data collection prevented seeing the poleward boundary of the feature. Again, it is interesting to consider the possibility that this dark area is or was a lake or sea in the context of the Rannou *et al.* (2006) GCM model. This model predicts that high-latitude regions on Titan are likely to be saturated, such that surface liquids may persist for long periods. The model predicts, and observations during Titan's southern midsummer have observed, methane storms at 70°S and poleward. Thus a paradigm emerges of wet polar regions (albeit somewhat distinct from that considered by Stevenson and Potter (1986)).

3.3 Aeolian Features

No dunes were observed in T7: these linear, radar-dark features were observed in several large (hundreds of km) patches in T3, and were suspected to be aeolian in origin (Elachi *et al.* 2006).However, the T8 swath, over a near-equatorial area known to be optically dark, found aeolian features in striking abundance. As documented in Lorenz *et al.* (2006), over half the swath was occupied by linear (longitudinal) dunes, very similar in size and morphology to those found on Earth in the Arabian and Namib deserts. In much of the swath the high viewing geometry (orthogonal to the long axes of the dunes) permitted topographic shading to appear, suggesting dune heights of ~150m and slopes (averaged over ~350m pixels) of about 6°.

The longitudinal nature of the dunes is evident from their interaction with other topography – the dunes break around and rejoin beyond topographic obstacles such as the hills or mountains on the eastern end of T8. Such a morphology requires a fluctuating (typically bidirectional) wind regime – Lorenz *et al.* (2006) suggest that the gravitational tidal winds modeled by Tokano and Neubauer (2002) may be responsible for the variation, although the general trend of the dunes is eastwards, consistent with the zonal winds at high altitudes. A systematic mapping of the dune orientation in future work will be an important constraint on Titan's wind meteorology. It is already apparent that there are regional deviations from the generally eastward trend, in some cases by as much as 30 degrees. In most cases these deviations can be attributed to the influence of nearby topography, and in one prominent case, a set of transverse dunes appear where a topographic obstacle appears to 'straighten' the fluctuations in flow direction.

The dunes appear superposed on all other features, suggesting they are young. It is estimated (Lorenz *et al.* 2006) that formation times may be as short as a few thousand years, similar to terrestrial dunes. Optically dark (and radar-dark) areas at low latitudes often appear to be associated with dunes or cat-scratches. However, at higher latitudes thus far observed, dark regions are apparently due to something else – either sand sheets not sculpted into dunes, or perhaps liquid deposits.

3.4 Hills

Features with high topography above surrounding terrain within the T7 swath are a low cluster of hills at the northwestern end of the swath and high plateaus within the middle, radar-bright, dissected region. The northern hills are most likely the remnants of a partially buried, eroded structure, perhaps a sub-circular volcanic ring or impact crater. However, the structure is so eroded that it is difficult to confidently propose any particular mechanism for its origin. The central, radar-bright region contains channels that appear to have cut down through underlying materials. There is some evidence of

topography in the form of bright/dark pairing associated with the channels, perhaps similar to the channeled regions seen by Huygens DISR near the landing site (Kirk *et al.* 2005), but on a much larger spatial scale. The gradation southward to channels that show no evidence of topography suggests something crudely analogous to the Colorado Plateau, in which rivers erode through bedrock, leaving steep cliffs that grade to gentle alluvial fans.

The eastern end of the T8 swath, just west of the Huygens landing site, contains long chains of features demonstrating high topography through radar shading that have been described as mountains (Radebaugh *et al.* in review). These features are curvilinear in planform, have an overall E-W orientation, and form ranges that extend several hundred kilometers. They have a strong appearance of having experienced erosion, both in their disconnected and dissimilar summits and in the light colored, diffuse materials (perhaps erosional blankets) that surround the mountains. Strong bright/dark pairing between the mountain summits enabled us to use radarclinometry to calculate slopes and heights of various peaks within the ranges. Maximum mountain heights are just over 600 m (with a mean of 240 m) above their surrounding blankets, and mean 90th percentile maximum slopes are close to 10 degrees (Radebaugh *et al.* in review). The curvilinear morphology of these ranges indicates they may have formed through tectonism. Localized compression of the crust is a possibility, due to the thickening of Titan's water ice crust associated with general cooling or, very recently, the onset of crustal convection (Tobie *et al.* 2006).

3.5 Circular features: impact or cryovolcanic?

Bright-rimmed, dark floored circular features are common in the T7 swath (see the figures in Wood et al., 2006). Their diameters are generally only 5-10 kilometers, at or below the limit expected based on the screening effect of the present-day atmosphere (Lunine et al., 2005), with one as small as 3.5 km (Wood et al., 2006). Each feature is poorly resolved but as a class they seem distinctive. The features are quite round and often have narrow bright rims. More than 500 circular features were observed in the T8 mountains region, covering 800 x 200 km. They present a dark center with brighter rims with a diameter ranging between 1 and 2 km, and a steep decline toward higher diameters. T8 is not the first swath in which such features are found; a few may be present in T3 data (Elachi et al., 2006).

Two hypotheses can be proposed to explain the origin of these features: impact craters or hydrothermal vents related to cryovolcanism. The general paucity of much larger and hence more readily recognizable impact craters on Titan (Elachi et al., 2006), and the improbable size distribution of these features (impactors responsible for craters of this size, 1-2km, should not be able to pass through the atmosphere without breaking up given the column density of Titan's atmosphere; Lunine et al., 2005), argues against a primary impact origin, and the absence of larger features nearby that could be interpreted to be impact craters rules out origin from secondary impacts.

There is no distinctive morphology that argues in favor of impact versus cryovolcanism as the origin of these features. If they are impact craters they are heavily weathered; arguments in favor of a cryovolcanic origin are hampered by the lack of

apparent flows exuded from the craters in contrast to similar features seen in the Ta swath (Elachi et al., 2005), with the exception of one possible flow associated with a crater in T8 (Lopes et al; 2006). However, methane released from a subsurface reservoir hundreds of meters under the surface might lead to fluidized sediments and/or ice expulsion along conduit tubes terminating at Titan's surface as numerous circular structures. Analogous structures exist on the Earth formed with water as the working fluid (Svenson et al., 2003). Whether such a process would work on Titan and what would be the underlying geologic process in the crust of Titan require detailed modeling beyond the scope of this paper; we suggest this as a possible explanation for a population of circular structures worthy of further investigation.

4. Radiometry, altimetry, and relationship to Ta-T3 mapped units
4.1 Radiometry

Radiometry was obtained in all modes, inbound and outbound. The radiometry independently addresses dielectric composition, surface and subsurface scattering properties, and is diagnostic of the relative roles of these properties in the radar appearance of different terrains. A broad region that was observed with combined scatterometry and radiometry in Ta (Elachi et al., 2005) was observed again in T8 in the orthogonal polarization. This region includes the Huygens probe landing area and the western portion of Xanadu. Preliminary results from the polarization dependence of the brightness are consistent with a surface with dielectric constant ~ 2 in the region of the landing site. However the Xanadu region appears to be virtually unpolarized radiometrically, which indicates an unusually rough or porous surface on the scale of the 2-cm wavelength. This region is also of relatively low radiometric brightness which, in combination with the polarimetry, implies increased subsurface scattering.

The dark area at the poleward end of T7 shows similar normalized radar cross section ("σ_0", expressed in decibels), and a brightness temperature a few degrees lower, than is observed for the dark dunes in T8 (Fig. 4), where statistics are derived from 6 sample areas of $4.9x10^3$ km² selected in each swath. This leads to the possibility that the dark, embayed, terrain might be a dry lake with infilling of organic material similar in composition and dielectric properties to the dunes, perhaps the reservoir of fine particulate material that is swept away and accumulated in the aeolian deposits mainly observed in the equatorial region of T8 and T3. Although a clear transition can be seen between the bright and dark terrains in SAR data, this is not shown in the radiometry data, which could suggest that the equatorward side of the embayment is the same material but is simply rougher on a scale of centimeters.

The SAR-bright terrains showing in T7 as hills and eroded terrains, and T8 as mountain chains and dome shaped features, show similar σ_0 and low brightness temperature similar to other areas imaged in the previous Ta and T3 swaths (Fig. 4). This would suggest that the bright eroded terrain in the lower latitude part of the T7 swath and the mountains and dome features in T8 might be characterized by material with higher dielectric constant (water-ammonia ice $\varepsilon=4.5$) than that further poleward in T7, or that high volume scattering is present and would in turn suggest SAR-bright and high σ_0 values due mainly to topographic effects. The model applied here to extract the calibrated

brightness temperature uses a dielectric value of 2 for organic materials (Janssen, 2004; Paganelli et al., 2006).

4.2 Scatterometry

Low-resolution radar reflectivity (scatterometer) data were recorded on both T7 and T8 passes, however the T7 data were in a compressed format that is not well calibrated. Data acquired on the inbound segment of T8 overlap significantly with the inbound pass of Ta, and reproduce it closely. Fits of scattering models consisting of a Hagfors-like specular term plus a $\cos^n$ diffuse component yield a dielectric constant of 2.3+/- 0.15 and a surface roughness of 5-6° rms slope. This dielectric constant is too low for all but the least consolidated water ice, and more consistent with mixtures of organic materials or even CO_2 ice. The outbound T8 pass data suggest a higher dielectric constant (~3.6) and rougher surface (10° rms).

4.3 Altimetry
Altimetry

Altimetry measurements for T7 were lost due to the on-board recorder anomaly, while altimetry data were successfully collected both before and after the T8 SAR pass. The T8 inbound altimetry swath spans approximately from 170° W to 180° W, almost exactly on the equator. It lies in the infrared-dark region Shangri-La, about 700 km north-east of the Huygens landing site. The outbound pass is also very close to the equator, extending from 310°W to 320°W, and is located in another dark region, Senkyo. No regional slopes or large-scale features can be observed, and the variation of topographic heights along the ground track is modest, with a standard deviation of 20-30 meters in both topographic profiles, which were respectively 400 and 500 km long. This value is comparable to the 30 m vertical resolution of the altimeter. For comparison, Schenk and Pappalardo (2004) report a standard deviation of 77 m over a 200 km long topographic profile across Conamara Chaos on Europa. Values of 10-20 m for the standard deviation over 30 km-long topographic profiles are typical for the Vastitas Borealis formation on Mars (e.g. Orosei et al. 2003).

It has been discovered that most of Shangri-La, as well as Belet, are covered in large fields of longitudinal sand dunes, with typical spacing of a few km and heights of 100-150 m (Lorenz et al., 2006). Topographic profiles across such dunes would have a standard deviation of the order of 50 m, but because the altimeter echo averages the topography over an area which is at least 20 km across (Callahan et al., in preparation), the footprint-to-footprint height variation along the ground track of the altimeter is probably inadequate to derive the rms height of any dunes existing in the observed area.

Preliminary work to use range-centroid correction in the SAR data to obtain elevation changes along the SAR swaths themselves suggest a progressive downward trend in elevation from the equatorial to the polar end of the T7 swath (Stiles *et al.* to be in preparation).

4.4 Relationship of T7 and T8 areas to mapped units in Ta and T3

The bulk of the T7 swath (Fig. 5) consists of a unit with a variable radar appearance, similar to the mottled unit seen in the Ta and T3 swaths (Stofan et al., 2006).

This unit has been interpreted to be a "plains" unit of unknown origin, likely largely composed of a spatially varying mixture of ice and organics. The hilly bright terrain at the equatorward end of the T7 swath is mapped as a bright rough unit, also present in the T3 swath. In the center of the swath, a bright mottled unit and a bright homogenous unit are mapped, and again are seen in the T3 swath. The scalloped edge unit near the southern end of the swath is mapped as a patchy unit, and has a morphology not seen previously in any other swath. The southern end of the swath is mapped as a homogeneous unit, similar to expanses of dark, relatively uniform terrain in Ta and T3, though this unit does appear to have lower backscatter.

The channels are confined to the region south of the small gaps in the T7 swath, and are superposed on the mottled unit, the bright mottled unit, the bright homogenous unit and the patchy unit. In previous regions mapped (Stofan et al., 2006), channels tended to be more specifically located near geologic features, such as Ganesa Macula in Ta and Menrva Crater in T3. Mapping of channels in the T7 swath indicates their ubiquity over much of the swath, with the exception of the mottled plain-type unit at the northern end and the very dark homogenous unit at the southern end. The lack of similarity of the patchy unit to other units, and its close association with the 'shoreline' and channels, does suggest that it is a topographically higher region that has been dissected and eroded by fluvial processes.

Mapping of the T8 region (Fig. 6) also reveals units seen in other regions of Titan. The central, radar-dark portion of the swath can be classified as the homogenous unit identified in Stofan et al. (2006), bounded on the eastern and western sides by the bright mottled unit. Both of these units have superposed dunes. Both ends of the swath have linear to curvilinear, irregular outcrops of the bright rough unit, representing relatively higher terrain (the 'mountains' described above) that has either been extensively eroded and/or buried. The features at the western end of the swath are less distinct, and appear to be more degraded. It is possible that material derived from these hills, for example through one of or a combination of fluvial-, rainfall-, and aeolian erosion onto tectonically weakened ices, provides much of the fine-grained debris found in the dunes. . The chains of hills appear somewhat sinuous, more suggestive of features produced by compression than those produced by extension (Radebaugh et al., 2006). In the T8 case, the bright mottled unit does appear somewhat different than that mapped in other regions, in that it is predominantly composed of bright, patchy materials in close association with the linear hills. In this case, the mottling is likely due to variable roughness and extent of the blankets surrounding, and perhaps shed from, the hills.

In summary, mapping of the T7 and T8 swath reveals that much of the landscape covered in these radar swaths contains morphologic units similar to those mapped in earlier swaths, but with differences in their distributions and relationships. For example, patches of the bright rough unit were mapped in the T3 swath, but they do not form the more coherent sets of hills mapped in T8. We see no strong evidence of the cryovolcanic units of the Ta swath in T7 and T8, other than the enigmatic circular features discussed above. Additionally, dune fields in T8 are much more extensive and coherent than those seen in T3. The similarities between the basic morphologic units of the swaths suggest we are seeing regions formed by similar processes (aeolian, fluvial, cryovolcanic, limited tectonic), but the relative significance of each process varies, across different local and regional areas and perhaps over time.

5. Location of the landing site of the Huygens probe in T8

Location of the Huygens probe's landing site on Titan's surface was accomplished by comparing the T8 Radar image with the DISR image observations. The first step in this process was to prepare a mosaic from the DISR images with the same projection and scale on Titan's surface as existed for the T8 Radar swath. This mosaic is shown as an inset to Fig. 7. This circular area has a diameter of about 90 km on Titan's surface.

The next step was to constrain the area of potential landing sites by performing a dispersion analysis of the Descent Trajectory Working Group's (DTWG) calculation of the impact latitude and longitude. The DTWG analysis was primarily an integration of the measured probe accelerations for two cases: 1) from the atmosphere interface point at 1270 Km (as determined by JPL) downward and 2) from Titan's surface upward. The lower trajectory was then tied to the upper trajectory near 150 Km altitude. In the lower atmosphere wind measurements were also included in the analysis. The red ellipse in Fig. 7 shows the limits of the DTWG analysis dispersion.

Once the general area on the T8 swath had been determined a detailed search of this region was performed in an attempt to locate prominent features from the DISR mosaic on the T8 map. Several locations were evaluated, however the field was quickly reduced to 4 possible sites. These are shown by the numbers and ghost mosaic outlines in Fig. 7. The primary characteristic of interest was a dark colored area between lighter regions representing a possible southwest to northeast flow field. Site #1 is the best fit to the DISR data because of the matching of 4 additional prominent features: two horizontal features to the north (likely dunes), a circular feature near the top center, and the diagonal 'shoreline' near the center, as indicated in Fig. 8.

The Huygens probe's final resting place was determined on the mosaic via analysis of the DISR image progression to better than 100 meters accuracy. Consequently its position can be subscribed on the Radar swath thus indicating the probe's landing site.   Fig. 9 shows the T8 Radar swath overlaid with the DISR mosaic. Instrument sensitivity variations and geometric distortions degrade the registration accuracy between the DISR mosaic and Radar map to perhaps a few kilometers. We hope to be able to improve the accuracy using data from later encounters. The resulting coordinates for the Huygens landing site are 192.4 degrees W longitude and -10.2 degrees N latitude (that is, south of the equator) to an accuracy of about 0.1 degree.

6. Interpretations and unresolved questions for future observations.

The two areas on Titan covered by the T7 and T8 passes are very different from each other, and underscore the strong diversity of Titan's landscapes. T7 imaged an area where liquids have dissected or are dissecting a landscape that likely has an overall decline in elevation toward the South Pole. The dark, almost featureless area nearest the pole lacks dunes and has a relationship between radiometric brightness and surface reflectivity opposite that of other radar-dark expanses (principally dunes) imaged in other flybys. Whether this plain is covered by hydrocarbon (methane or ethane) liquid, or represents the equatorward edge of solid substances that are poorly represented in mid-latitude dune fields and other dark areas, is unclear. There is a net poleward transport of relatively volatile organic products of Titan's photochemistry, so there is a tendency over

time to accumulate solids of these products near the poles (Rannou *et al.* 2006), perhaps forming glaciers that slowly flow equatorward (Brown *et al.* 2006). If the polar temperatures are several degrees below the equatorial value of approximately 94 K, methane will preferentially rain out seasonally at the poles as well. The fine fluvial features seen toward the equatorial end of the pass and the more amorphous broad channels closer to the pole, may also play a role in feeding liquid to the dark basin, though in the absence of a rainfall rate it is difficult to predict how much. In either case, it is likely that the high-latitude, dark area of T7 is a unique unit not seen at lower latitudes.

The T8 landscape illustrates two important points about Titan surface processes. First, dune fields are abundant near the equator as seen in the T8 swath, and while dunes appear at higher latitudes, in the areas imaged by radar to date, they are less well defined—perhaps because of a relative lack of sand-sized particles or of the appropriate wind fields. Second, the overall lack of significant (> 1 km amplitude) topography and appearance of subdued features hints either at a thin crust or deep burial of features over large areas of the T8 swath.

Suppose Titan's surface were, on average, roughly a billion years old, based on the small number of identified impact craters (and whether or not the ambiguous candidates discussed above in T7 and T8 are included). Photochemical models predict that the solid component of the stratospheric photochemical debris produced over geologic time (that is, excluding the ethane which is liquid under current Titan conditions) is equivalent to a globally-averaged layer only 100-200 meters thick (e.g., Wilson and Atreya, 2004). If we assume that large-scale resurfacing events that have acted to erase craters formed prior to a billion years ago also mixed some of this solid photochemical debris into the ice crust, then the amount of photochemical sediment available to bury geologic features might be less than 100 meters thick, globally averaged, at present. The radarclinometric height of the mountains in T8 is on average 200 meters (Radebaugh et al. 2006); the topographic amplitude of the structures in total might be then be not much more than this even if their bases and parts of surrounding blankets are covered in photochemical debris. Thus the mountains on Titan are quite different from, for example, the Basin and Range structures in the southwestern part of North America, where much of these structures are buried under kilometers of sediments.

On the other hand, there is an apparently equally self-consistent argument, that hinges on a much deeper layer of <u>solid</u> photochemical debris being present over Titan's surface than is predicted by the standard photochemical models. Were Titan's surface blanketed by many hundreds of meters of such organic sediments, it might be possible that a large number of craters are obscured by burial across a surface that is, in fact, many billions of years old. The mountains observed in T8 might then have much larger total topographic amplitudes—a kilometer or more—implying a relatively thick lithosphere.

If future radar and other remote sensing observations support the argument that the topographic amplitude in the T8 region is limited to just a couple of hundred meters, it could set a useful limit on the lithospheric thickness for the period in Titan's history when these features formed if relaxation (as opposed to erosion) is the dominant process in removing topography. Calculating the effect of relaxation on topography is difficult because of the poorly known rheological properties of extremely cold water ice, variants such as methane clathrate hydrate, and the thermal gradients in the crust. One thermal evolution model posits a thin (10 km or less) crust for much of Titan's history,

maintained by the insulating and high-viscosity properties of methane clathrate hydrate, and thickening to 60 km only in the last ~ 500 million years as declining heat flows encourage the formation of normal ice I (Tobie *et al.* 2006). Thus only features of order this age or less will exhibit significant topographic amplitude, and thus in the T8 region much of the geology may be older than a half billion years, with the exception of the mountain chains that appear to be younger, based on other analyses (Radebaugh *et al.* 2006).

Future Cassini radar opportunities are limited by the number of flybys and competition with other instruments—none of which are bore sighted with the radar. Where flexibility exists in choosing either to fly over the same area at a different azimuth or to cover new territory, a natural tension exists. The absence of dunes in the T7 dark area could theoretically be an artifact of the different illumination azimuth of this north-south pass relative to that used for the east-west Ta, T3 and T8 passes. It is therefore important to cover at least some of the T7 dark area at a perpendicular illumination azimuth to search for dunes. Extending the coverage of the dark area closer to the pole—where more methane or ethane liquid could be present—is important as well. With respect to resolving the question of impact, cryovolcanic, or other origin of the circular features in T8, little can be done with the resolution available, except perhaps to try stereo imaging of features again by passing over the region at a different illumination azimuth. Perhaps a better approach to this is more coverage of Titan to refine locations and associations, since some circular features are seen in other regions, e.g. in the T3 swath. Higher resolution coverage of the Huygens site—300 meters instead of a kilometer—would also be of help. Finally, if the radar dark area near the high latitude end of the T7 swath contains liquid, it is possible that the shoreline may migrate seasonally over many kilometers (Mitri et al., 2006), and hence will have a different shape in radar images taken late in the Cassini prime mission or a possible extended mission.

More broadly, the diverse terrains seen in T7 and T8 whet the appetite for more powerful radar systems or—in the long-term—a balloon-borne payload that would obtain Huygens-resolution near-infrared imaging (1-10 meters) over large swaths of Titan's surface (Lorenz *et al.* 2005; Lorenz and Tokano, 2006).

Table 1. Swath characteristics.

	T7	T8
Resolution range, km	0.3-0.8	0.3-1.2
Acquisition date	7-9-05	27-10-05
Swath length, km	1970	5000
Latitude Range, °	31-70 S	11-7 S
Longitude Range, °	23W-11E	186-314 W
Inclination angle range, °	15-30	17-23

References

Elachi, C., Wall, S., Allison, M., Anderson, Y., Boehmer, R., Callahan, P., Encrenaz, P., Flamini, E., Francescetti, G., Gim, Y., Hamilton, G., Hensley, S., Janssen, M., Johnson, W., Kelleher, K., Kirk, R., Lopes, R., Lorenz, R., Lunine, J., Muhleman, D., Ostro, S., Paganelli, F., Picardi, G., Posa, F., Roth, L., Seu, R., Shaffer, S., Soderblom, L., Stiles, B., Stofan, E. Vetrella, S., West, R., Wood, C. , Wye, L. and Zebker, H. 2005. First views of the surface of Titan from the Cassini RADAR. Science 308, 970-974.

Elachi, C., Wall, S. Janssen, M., Stofan, E., Lopes, R., Kirk, R., Lorenz, R., Lunine, J., Paganelli, F., Soderblom, L., Wood, C., Wye, L., Zebker, H., Anderson, Y., Ostro, S. Allison, M., Boehmer, P. Callahan, P., Encrenaz, P., Flamini, E., Francescetti, G., Y. Gim, Y.,Hamilton, G., Hensley, S., Johnson, W., Kelleher, K., Muhleman, D., Picardi, G., Posa, F., Roth, L., Seu, R., Shaffer, S., Stiles, B., Vetrella, S., and West, R. 2006. Titan Radar Mapper Observations from Cassini's T_3 Flyby. Nature 441, 709-713.

Kirk, R. L., B. A. Archinal, M. G. Tomasko, B. Rizk, L. A. Soderblom, D. A. Cook, E. Howington-Kraus, T. L. Becker, M. R. Rosiek, and the DISR Science Team 2005. Topographic Mapping of the Huygens Landing Site on Titan. Amer. Astronom. Soc. Div. Planet. Sci. Meeting 37, Abst. 46.08.

Lemouelic, S., Rodriguez, S., Stephan, K., Scholz, C. K. 2005. Release of volatiles from a possible cryovolcano from near-infrared imaging of Titan. Nature 435, 786-789.

Lopes, R., K. L. Mitchell, E. R. Stofan, J. I. Lunine, R. Lorenz, F. Paganelli, R. L. Kirk, C. A. Wood, S. D. Wall, L. E. Robshaw, A. D. Fortes, C. D. Neish, J. Radebaugh, E. Reffet, S. J. Ostro, C. Elachi, M. D. Allison, Y. Anderson, R. Boehmer, G. Boubin, P. Callahan, P. Encrenaz, E. Flamini, G. Francescetti, Y. Gim, G. Hamilton, S. Hensley, M. A. Janssen, W. T. Johnson, K. Kelleher, D. O. Muhleman, G. Ori, R. Orosei, G. Picardi, F. Posa, L. E. Roth, R. Seu, S. Shaffer, L. A. Soderblom, B. Stiles, S. Vetrella, R. D. West, L. Wye, and H. A. Zebker. 2006. Cryovolcanic features on Titan's surface as revealed by the Cassini Titan Radar Mapper. Icarus, submitted.

Lorenz, R.D., Lopes, R., K. L. Mitchell, E. R. Stofan, J. I. Lunine, F. Paganelli, R. L. Kirk, C. A. Wood, S. D. Wall, L. E. Robshaw, A. D. Fortes, C. D. Neish, J. Radebaugh, E. Reffet, S. J. Ostro, C. Elachi, M. D. Allison, Y. Anderson, R. Boehmer, G. Boubin, P. Callahan, P. Encrenaz, E. Flamini, G. Francescetti, Y. Gim, G. Hamilton, S. Hensley, M. A. Janssen, W. T. Johnson, K. Kelleher, D. O. Muhleman, G. Ori, R. Orosei, G. Picardi, F. Posa, L. E. Roth, R. Seu, S. Shaffer, L. A. Soderblom, B. Stiles, S. Vetrella, R. D. West, L. Wye, and H. A. Zebker 2006. Fluvial features on Titan, Icarus, submitted.

Lorenz, R. D., Elachi, C., Stiles, B., West, R. A., Janssen, M. A., Lopes, R. M., Stofan, E. R., Paganelli, F., Wood, C. A., Kirk, R. L., Lunine, J., Wall, S. D. 2005. Titan's

Elusive Lakes? Properties and Context of Dark Spots in Cassini TA Radar Data. Lun. Planet. Sci. Conf. 36, Abs. 1682.

Lorenz, R.D,, Wall, S., Radebaugh, J., Boubin, G., Reffet, E., Janssen, M., Stofan, E., Lopes, R., Kirk, R., Elachi, C., Lunine, J., Paganelli, F., Soderblom, L., Wood, C., Wye, L., Zebker, H. Anderson, Y., Ostro, S., Allison, M., Boehmer, R., Callahan, P., Encrenaz, P., Ori, G.G., Franceschetti, G., Gim, Y., Hamilton, G., Hensley, S., Johnson, W., Kelleher, K., Muhleman, D., Picardi, G., Posa, F., Roth, L., Seu, R., Shaffer, S., Stiles, B., Vetrella, S., Flamini, E., and West. R. 2006. The sand seas of Titan: Cassini RADAR observations of longitudinal dunes. Science 312, 724-727.

Lorenz, R.D., Zimmerman, W. and Lunine, J.I. 2005. Post-Cassini exploration of Titan: science goals, instrumentation and mission concepts. Adv. Space Research 36, 281-285.

Lunine, J., Artemieva, N., Lorenz, R., and Flamini, E. 2005. Numerical modeling of impact cratering on Titan with implications for the age of Titan's surface. Lunar and Planetary Science Conference 36, abstr. 1504.

Mitri, G., Showman, A.P., Lunine, J.I. and Lorenz, R.L. 2006. Hydrocarbon lakes on Titan. *Icarus*, submitted.

Niemann H.B., Atreya, S.K., Bauer, S.J., Carignan, G.R., Demick, J.E., Frost, R.L., Gautier, D., Haberman, J.A., Harpold, D.N., Hunten, D.M., Israel, G., Lunine J.I., Kasprzak, W.T., Owen, T.C., Paulkovich, M., Raulin, F., Raaen, E., and Way, S.H. 2005. The composition of Titan's atmosphere from the GCMS on the Huygens probe, and implications for the origin of nitrogen and methane. Nature 438, 779-784.

Orosei, R., Bianchi, R., Coradini, A., Espinasse, S., Federico, C., Ferriccioni, A., Gavrishin, A.I. 2003. Self-affine behavior of Martian topography at kilometer scale from Mars Orbiter Laser Altimeter data. Journal of Geophysical Research Planets 108, 4-1.

Paganelli,F. , M.A. Janssen, R. West, B. Stiles, S.D. Wall, P. Callahan, R.M. Lopes[1], E. Stofan, R.D. Lorenz, J.I. Lunine , R.L. Kirk, C. Elachi, and the Radar Team 2006. Titan surface from Cassini RADAR SAR and radiometry data of the first five flybys. *Icarus*, submitted.

Radebaugh, J., R. Lorenz, R. Kirk, J. Lunine, and the Cassini Radar Team. Mountains on Titan observed by Cassini Radar. Icarus, submitted.

Rannou, P., Montmessin, F., Hourdin, F., and Lebonnois, S. 2006. The Latitudinal Distribution of Clouds on Titan. Science 311, 201-205.

Schenk, P.M., Pappalardo, R.T., 2004. Topographic variations in chaos on Europa: Implications for diapiric formation. Geophys. Res. Lett. 31 doi:10.1029/2004GL019978.

Sotin, C., Jaumann, R., Buratti, B. J., Brown, R. H., Clark, R. N., Soderblom, L. A.,

Baines, K. H., Bellucci, G., Bibring, J.-P., Capaccioni, F., Cerroni, P., Combes, M., Coradini, A., Cruikshank, D. P., Drossart, P., Formisano, V., Langevin, Y., Matson, D. L., McCord, T. B., Nelson, R. M., Nicholson, P. D., Sicardy, B., Stevenson, D.J. and Potter, B. E. 1986. Titan's latitudinal temperature distribution and seasonal cycle. Geophys. Res. Letters 13, 93-96.

Stofan, E., Lunine, J.I., Lopes, R., Paganelli, F., Lorenz, R., Wood, C., Kirk, R., Wall, S., C. Elachi, M. D. Allison, Y. Anderson, R. Boehmer, G. Boubin, P. Callahan, P. Encrenaz, E. Flamini, G. Francescetti, Y. Gim, G. Hamilton, S. Hensley, M. A. Janssen, W. T. Johnson, K. Kelleher, D. O. Muhleman, G. Ori, R. Orosei, G. Picardi, F. Posa, L. E. Roth, R. Seu, S. Shaffer, L. A. Soderblom, B. Stiles, S. Vetrella, R. D. West, L. Wye, and H. A. Zebker. 2006., Mapping of Titan: results from the first two radar passes. Icarus, submitted.

Svensen, H., Planke, S., Jamtveit, B. and Pedersen, T. 2003. Seep carbonate formation controlled by hydrothermal vent complexes: A case study from the Voring Basin, the Norwegian Sea, Geo-Mar Lett. 23, 351-358.

Tobie, G., Lunine, J.I., Sotin, C. 2006. Episodic outgassing as the origin of atmospheric methane on Saturn's moon Titan. Nature 440, 61-64.

Tokano, T. and Neubauer, F.M. 2002. Tidal Winds on Titan Caused by Saturn. Icarus 158, 499-515.

Tokano, T. and Lorenz, R.D. 2006. GCM simulation of balloon trajectories on Titan. Planetary and Space Science 54, 685-694.

Tomasko, M., Archinal, B., Becker, T., Bézard, B., Bushroe, M., Combes, M., Cook, D., Coustenis, A. de Bergh, C., Dafoe, L., Doose, L., Douté, S., Eibl, A., Engel, S., Gliem, F., Grieger, B., Holso, K., Howington-Kraus, E., Karkoschka, E., Keller, H., Kirk, R., Kramm, R., Küppers, M., Lanagan, P.,Lellouch, E., Lemmon, M., Lunine, J., McFarlane, E., Moores, J., Prout, M., Rizk, B., Rosiek, M., Rueffer, P., Schröder, S., Schmitt, B., See, C., Smith, P., Soderblom,L., Thomas, N., West, R. 2005. Rain, winds, and haze during the Huygens probe descent to Titan's surface. Nature 438, 765-778.

Wilson, E.H. and Atreya, S. 2004. Current state of modeling the photochemistry of Titan's mutually dependent atmosphere and ionosphere. J. Geophys. Res. 109 E06002, doi:10.1029/2003JE002181.

Wood, C.A., Lunine, J.I., Lopes, R.M., Stofan, E.R., Mitchell, K., and Radebaugh, J. 2006. Crateriform structures on Titan. Lunar and Planet. Sci. Conf. 37, abst. 1659.

Figure captions

Figure 1. Globes of Titan showing locations of Ta, T3, T7 and T8 data swaths. The swaths are superposed on globes composed of false color images from the Hubble Space Telescope. The top globe shows the Ta and T3 swaths, the middle globe shows the edge of the T3 swath and the T7 swath, and the bottom globe shows the T8 swath. North is up, and west longitude is used. See Table 1 for exact locations and dimensions of the T7 and T8 swaths.

Figure 2. Various views from the T7 SAR pass, shown progressively from the equator toward the pole.
  2a. Semi-circular pattern of hills. Image area is roughly 250km x 420 km.
  2b. Area in T7 cut by fairly extensive fluvial channel, fanning out into rougher (brighter) terrain. Image area is roughly 170 x 280 km.
  2c. Trace of one fluvial feature appears to run across the bright fan on the left, extending all the way across the 400 km length of the image.
  2d. Transition zone into a region of broader channels seen against a bright (rough?) background. Image 150x450 km, with resolution approaching 400 meters.
  2e. Most poleward and highest resolution part of the T7 swath, showing the transition from a scalloped terrain to a dark, almost featureless plain. Image size 150 x 490 km.

Figure 3. Various views from the T8 SAR pass, moving from west to east across Titan just south of the equator.
  3a. Relatively low (1 km) resolution view showing some poorly organized dunes, and dark, possibly fluid-filled, channels. Image area 300 x 600 km.
  3b. Onset of the well-organized dune fields near the center of T8, seen at very high (300-500 meter) resolution. Image size 150 x 1000km.
  3c. Dunes part and rejoin around obstructions, in the area east of the previous image. Image size 210 x 850 km.
  3d. Enigmatic terrain in which a series of ridges are interspersed with circular features of varying contrast. Area is 270 x 800 km.
  3e. Near the eastern end of the T8 swath, a large but faint circular feature is seen at low (1 km) resolution south of where another extensive dune field begins. Area 380x 440 km.

Figure 4. The cross section σ_0 is shown versus brightness temperature for T7 and T8 radar-bright (mountains) and radar-dark areas (embayment and dunes).

Figure 5(a). A map covering an approximately 700 km long region near the southeastern end of the T7 swath. Units mapped include the mottled unit, homogeneous unit, bright mottled unit, bright rough unit and patchy unit. Preliminary assignment of mapping units to T7. Key: bhu= bright homogeneous unit, bmu = bright mottled unit, bru= bright rough

unit, hu = homogeneous unit, mu= mottled unit, and pu= plains unit. Properties of all but the last of these, which was not previously seen, are reported in Stofan et al. (2006). The dashed lines indicate the location of channels. (b) Portion of the T7 swath covered in the map.

Figure 6. (a) This map covers an approximately 1000 km long segment of the T8 swath near its eastern end. The bulk of the area is mapped as the bright mottled unit, with small areas of the homogeneous unit at the western end. The stipple pattern marks the location of dunes; the unmarked units are the bright rough unit, demarking the position of hills. The pattern of the hills is suggestive of multiple orientations of long linear ridges, which have been subsequently eroded. North is to the top of the map. (b) Portion of the T8 swath covered by the map.

Figure 7. An excerpt from the T8 radar swath overlaid with the calculated Huygens descent landing ellipse in red, and showing the four primary landing sites under consideration. The inset shows a mosaic of the DISR images stretched, projected and scaled to match the radar's image to be used for comparison of features.

Figure 8. Similar to figure 7, but detailing the matching features from the radar and DISR data that were used in the final determination of the landing site of the Huygens probe.

Figure 9. An overlay of the DISR and Radar data showing the location of the Huygens probe landing site.
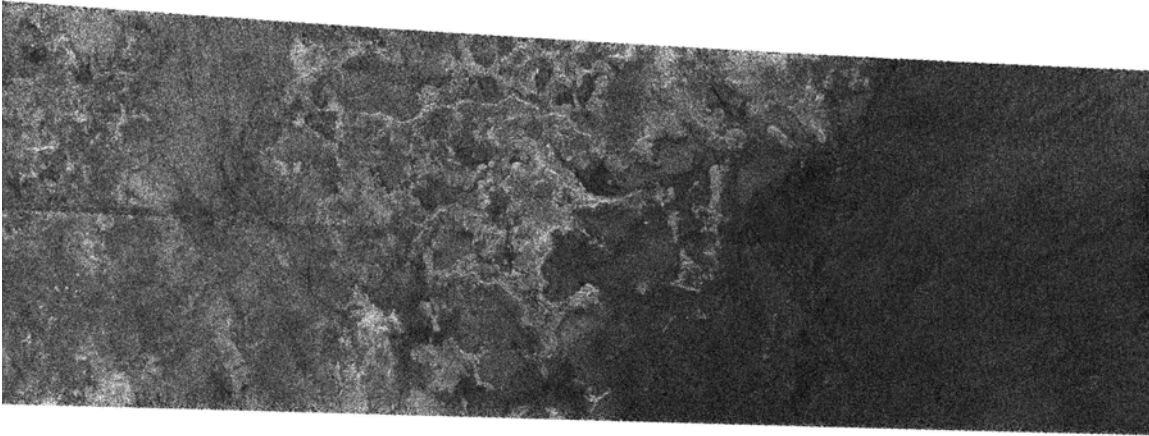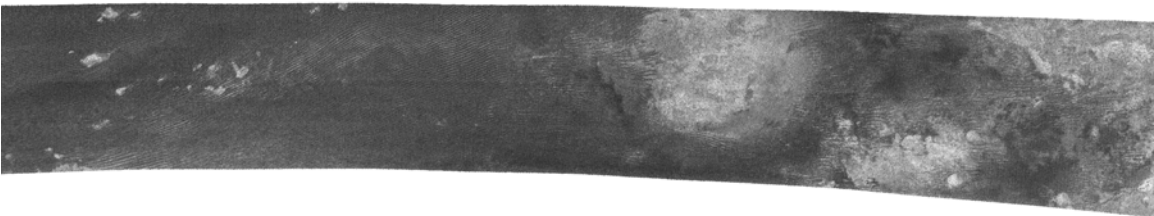
Figure 1
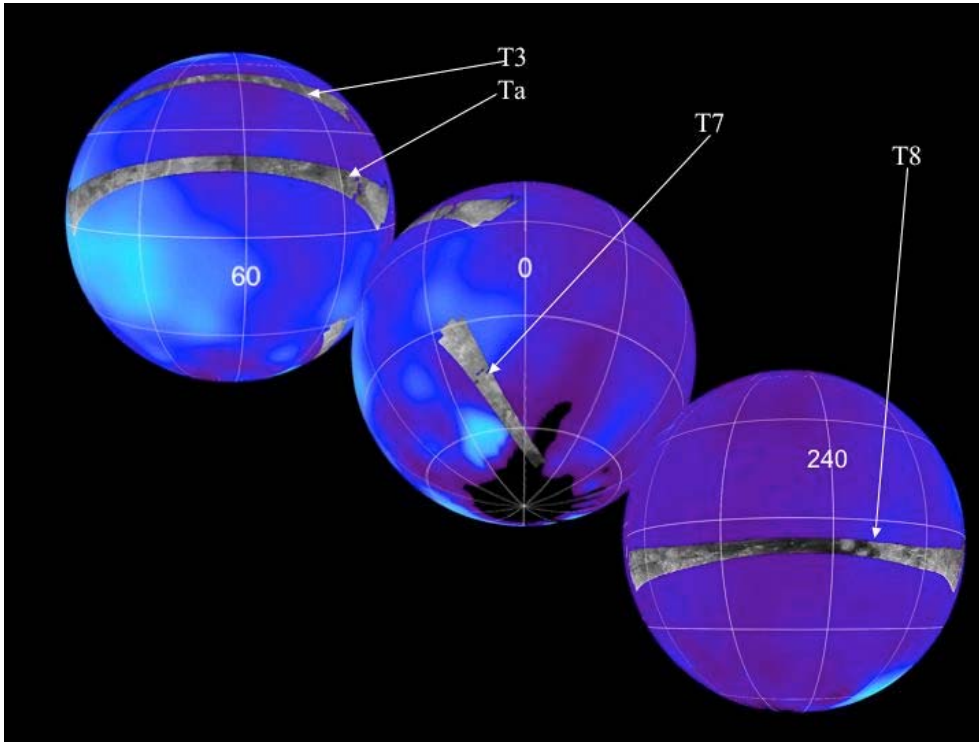
Figure 2
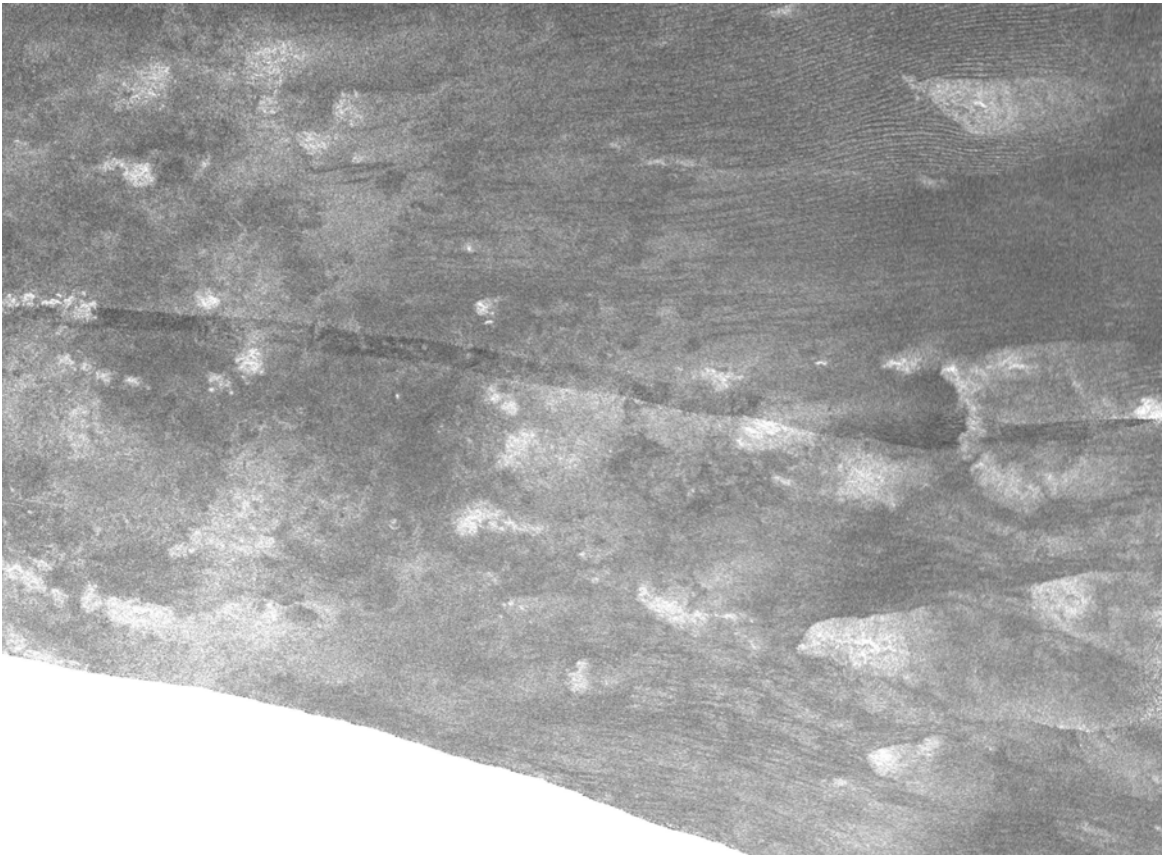
2a.
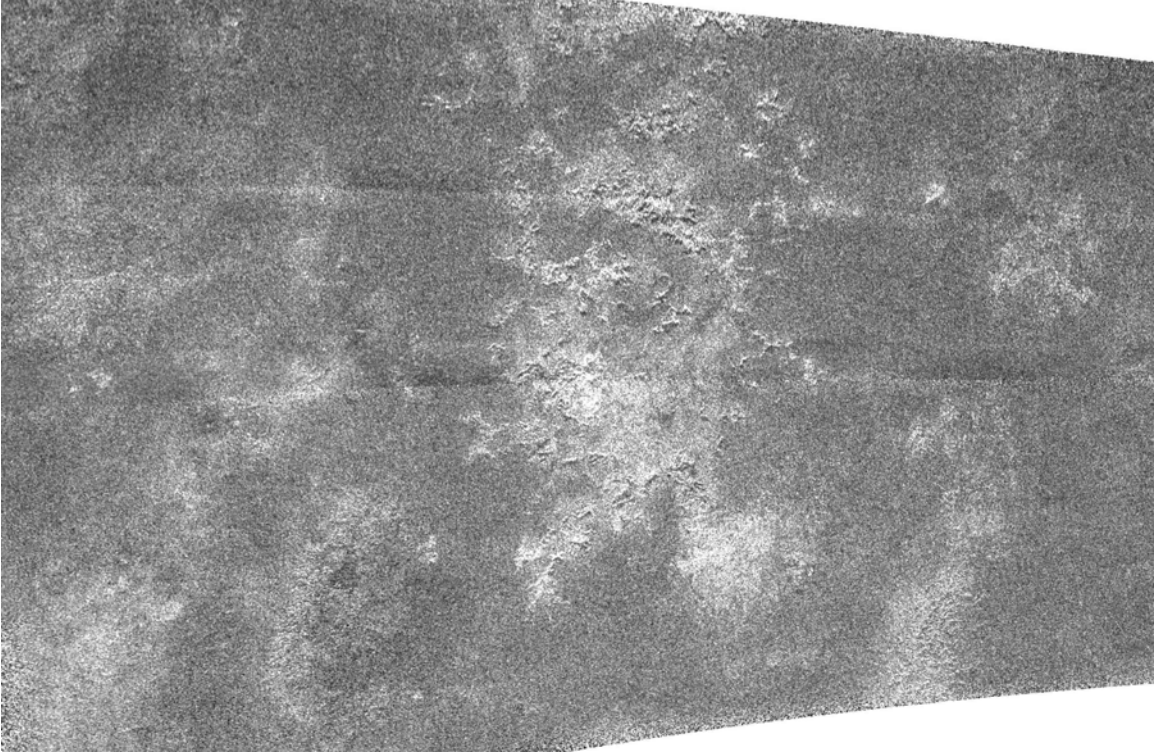
2b.

2c.
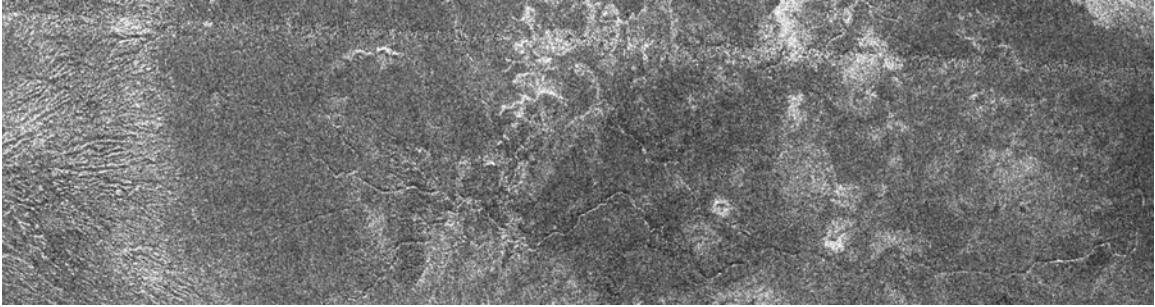
2d.
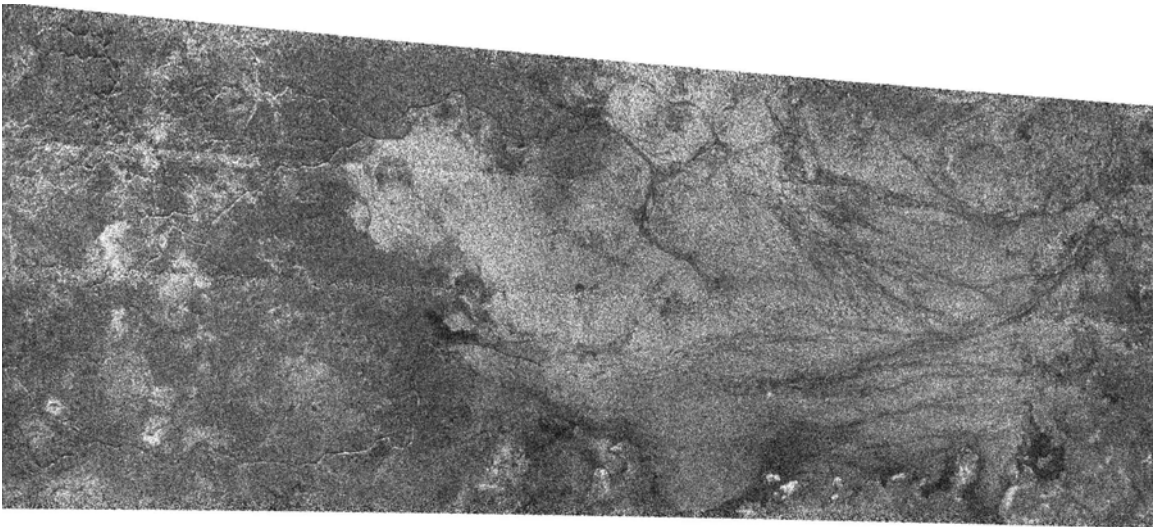
2e.
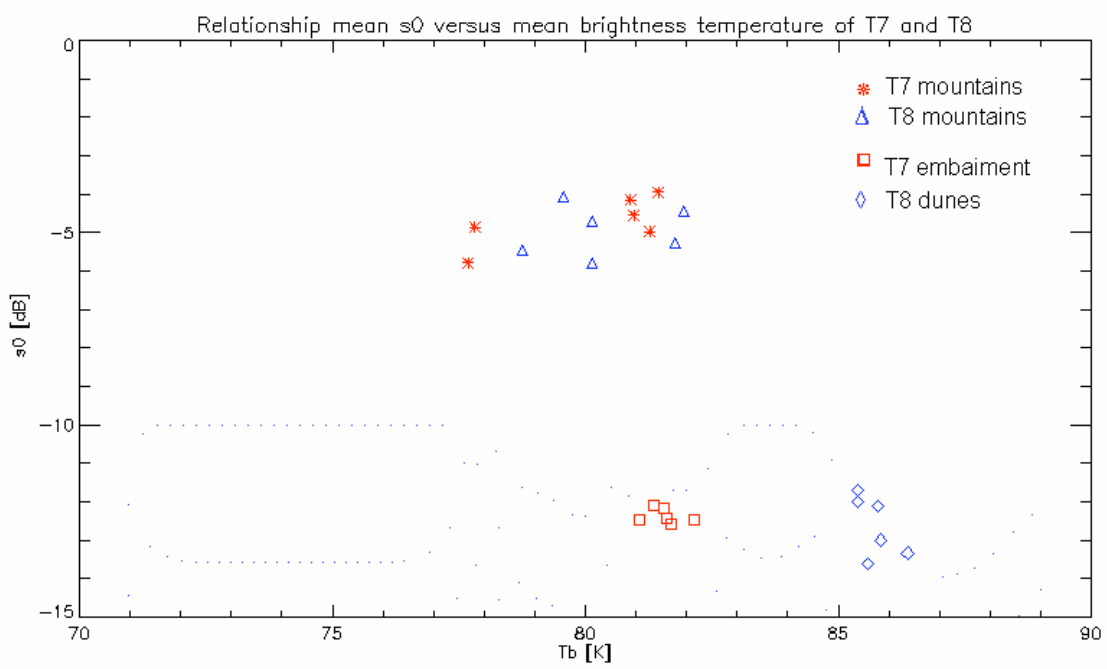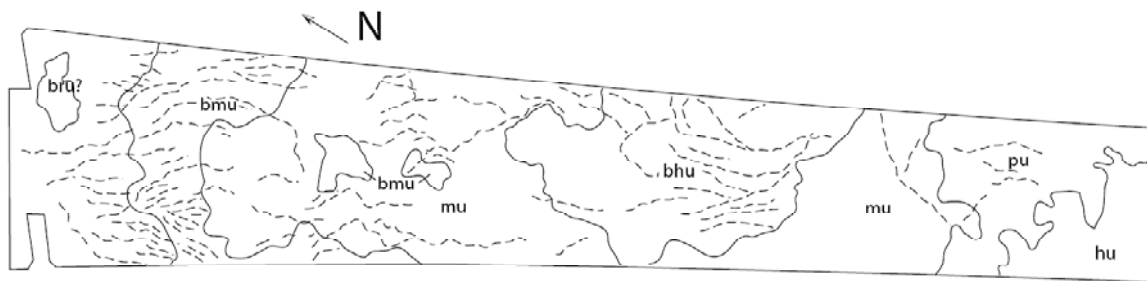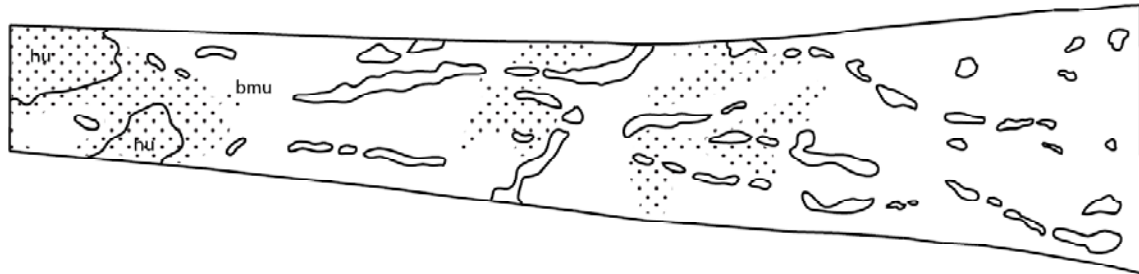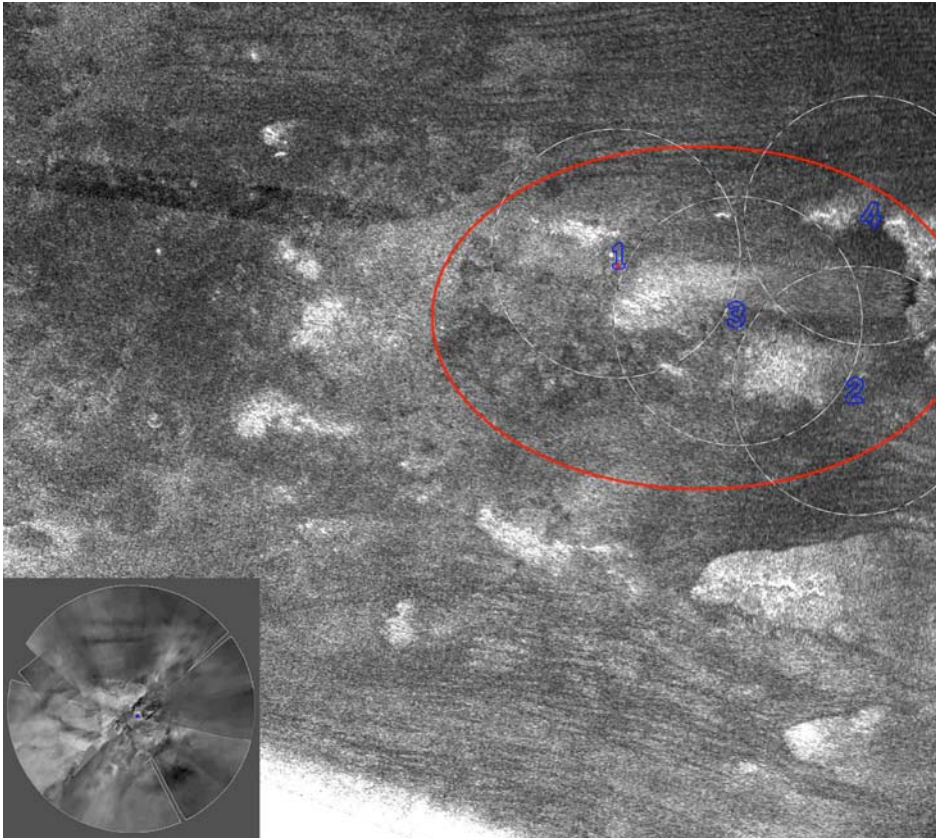
Figure 3.

3a.

3b.

3c.

3d.

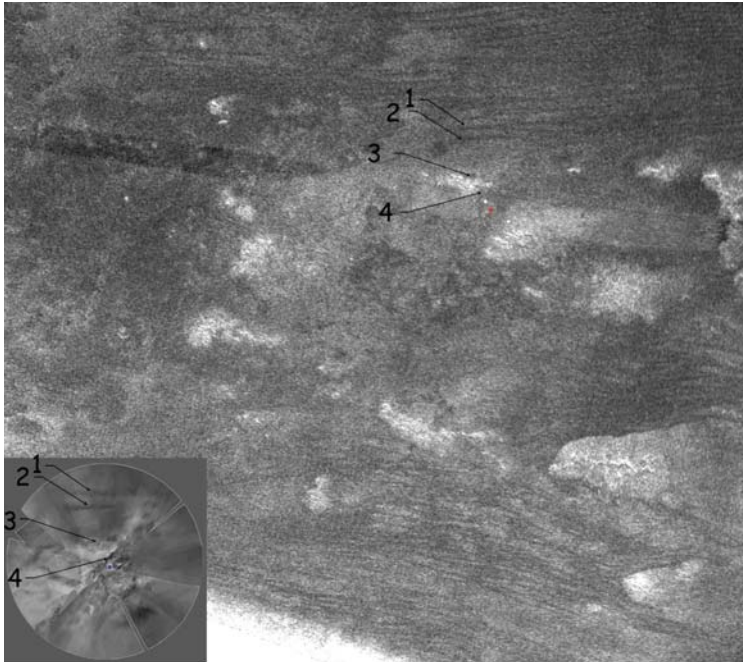3e.

Figure 4

5(a)

5(b)

Figure 5

6(a)

6(b)

Figure 6

Figure 7

Figure 8

Figure 9